Effect of Linker Segments on the Stability of Epithelial Cadherin Domain 2

Alka Prasad, Huaying Zhao, John M. Rutherford, Nicole Housley, Corey Nichols, and Susan Pedigo*
University of Mississippi, Department of Chemistry and Biochemistry, University, Mississippi

ABSTRACT **Epithelial cadherin is a transmembrane protein that is essential in calcium-dependent cell–cell recognition and adhesion. It contains five independently folded globular domains in its extracellular region. Each domain has a seven-strand β-sheet immunoglobulin fold. Short seven-residue peptide segments connect the globular domains and provide oxygens to chelate calcium ions at the interface between the domains (Nagar et al., Nature 1995;380:360–364). Recently, stability studies of ECAD2 (Prasad et al., Biochemistry 2004;43:8055–8066) were undertaken with the motivation that Domain 2 is a representative domain for this family of proteins. The definition of a domain boundary is somewhat arbitrary; hence, it was important to examine the effect of the adjoining linker regions that connect Domain 2 to the adjacent domains. Present studies employ temperature–denaturation and proteolytic susceptibility to provide insight into the impact of these linkers on Domain 2. The significant findings of our present study are threefold. First, the linker segments destabilize the core domain in the absence of calcium. Second, the destabilization due to addition of the linker segments can be partially reversed by the addition of calcium. Third, sodium chloride stabilizes all constructs. This result implies that electrostatic repulsion is a contributor to destabilization of the core domain by addition of the linkers. Thus, the context of Domain 2 within the whole molecule affects its thermodynamic characteristics. Proteins 2006;62:111–121.**

Key words: thermodynamics; calcium binding; modular domains; circular dichroism; thermal denaturation

INTRODUCTION

Cadherins are responsible for calcium-dependent cell–cell adhesion, facilitating tissue formation during morphogenesis.[1] Epithelial cadherins are single-transmembrane polypeptides that contain three distinct regions—a cytoplasmic region that connects to the cytoskeleton of the cell, a single-pass transmembrane region, and an extracellular region that is the location of calcium binding and protein–protein interactions that lead to cell adhesion.[2,3] The extracellular region comprises five individually folded domains. Solution[4,5] and crystallographic[6,7] studies show that the extracellular domains of epithelial cadherin are seven-strand β-barrel structures with the classic immunoglobulin fold. The most N-terminal domain (Domain 1) is known to participate in protein–protein interactions[8–12] and to undergo calcium-dependent conformational changes.[13] Calcium binds to residues in the β-barrel domains, as well as in the short peptide segments that link one domain to the other.[6,12] Calcium binding is essential for cell adhesion function[1,3,14] and changes the relative disposition of the extracellular domains.[13]

The long-term goal of research in our laboratory is to characterize the energetics of the various interactions in which the extracellular domains of cadherin participate. In particular, we are interested in the linkage between the folding, calcium binding, and assembly of the two-domain construct, ECAD12. This construct is surprisingly unstable in spite of the relative stability of the domains that comprise it (data not shown). Our approach is to dissect the global behavior of ECAD12 into the energetic contributions from each domain. Initial studies focused on the characterization of Domain 2 (ECAD2), which can be considered as a representative folding unit in epithelial cadherin.[15] Until recently,[12] this domain has not been implicated in dimerization or formation of higher order structures.[6,7,16] Since the definition of domain boundaries is somewhat arbitrary and can impact the thermodynamic characteristics of a domain, we explore in our present study the effect of adjoining linker segments upon Domain 2.

Abbreviations: BCA, bicinchoninic acid; BTEE, *N*-benzoyl-L-tyrosine ethyl ester; CD, circular dichroism; dATP, 2′-deoxyadenosine 5′-triphosphate; dNTP, deoxyribonucleoside triphosphate; ECAD12, epithelial cadherin domains 1 and 2; ECAD2, epithelial cadherin domain 2; ECAD2-L2, epithelial cadherin domain 2 + linker 2; EDTA, ethylenediaminetetraacetic acid; EGTA, ethyleneglycoltetraacetic acid; Ek/LIC, cloning vector from Novagen; GST, glutathione *S*-transferase; HEPES, *N*-2-hydroxyethylpiperazine-*N*′-2-ethanesulfonic acid; IPTG, isopropylthio-β-D-galactoside; LB, Luria–Bertani medium; L1-ECAD2, linker 1 + epithelial cadherin domain 2; L1-CAD2-L2, linker 1 + epithelial cadherin domain 2 + linker 2; MALDI-TOF, matrix-assisted laser desorption/ionization time-of-flight; MWCO, molecular weight cutoff; OD, optical density; PBS, phosphate-buffered saline; PCR, polymerase chain reaction; pI, isoelectric point; SDS-PAGE, sodium dodecyl sulfate–polyacrylamide gel electrophoresis; SEC, size exclusion chromatography; TE, 10 m*M* Tris/HCl, 1 m*M* EDTA, pH 8.

Grant sponsor: National Science Foundation; Grant number: MCB 0212669.

*Correspondence to: Susan Pedigo, Department of Chemistry and Biochemistry, University of Mississippi, University, MS 38677.
E-mail: spedigo@olemiss.edu

Received 22 December 2004; Accepted 19 May 2005

Published online 14 November 2005 in Wiley InterScience (www.interscience.wiley.com). DOI: 10.1002/prot.20657

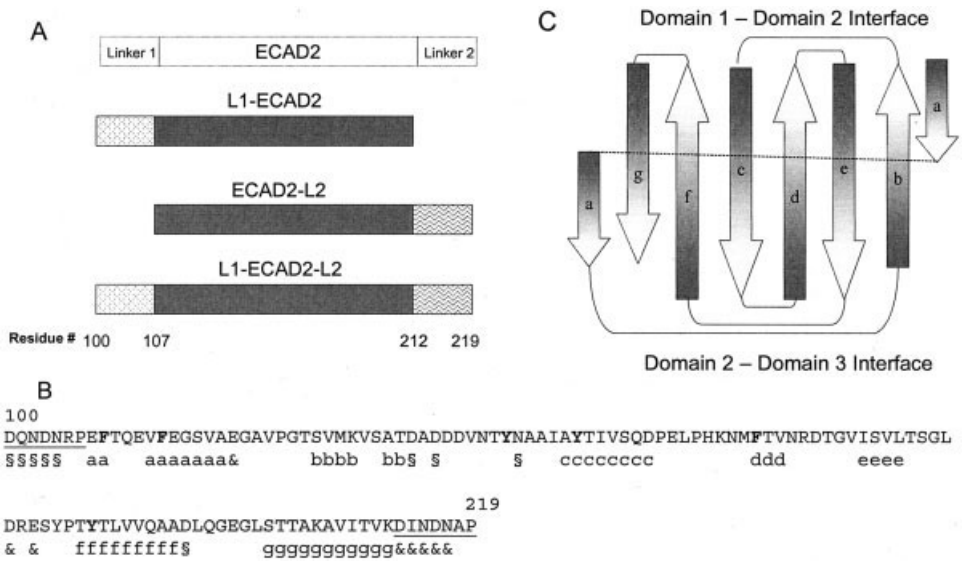

Fig. 1. Schematic and sequence of ECAD2, with and without adjoining linker segments. (**A**) Schematic of Domain 2 constructs. Nomenclature for each domain is noted. Residue numbers are noted along the bottom. Linker 1 is residues 100–106. Domain 2 is residues 107–212. Linker 2 is residues 213–219. (**B**) Amino acid sequence of Domain 2 with adjoining linkers segments. The seven residues of the linker segments are underlined, with Linker 1 at the N-terminus and Linker 2 at the C-terminus of the sequence for Domain 2. The amino acids are noted that contribute to the hydrogen bonding network for the seven strands (**a** through *g* in lower case under the amino acid sequence). The groups are designated that ligate the calcium between Domains 1 and 2 (§) and between Domains 2 and 3 (&) (based on Nagar et al.[6]). The possible cleavage sites for α-chymotrypsin are shown in bold. (**C**) Schematic diagram that illustrates the relative positions of the seven strands (a through g). The surface of the protein involved in the Domain 1–Domain 2 interface is shown. Residues marked (§) in (B) occur in the loop regions at this interface. The surface of the protein involved in the Domain 2–Domain 3 interface is shown. Residues marked (&) in (B) occur in the loop regions at this interface.

We defined the linker segments as follows: Each domain is a seven-strand β-barrel (strands a through g). The g-strand in each core domain is the longest of the seven strands and is terminated with a short conserved sequence, VITVX, where X represents any amino acid. The terminus of the g-strand is followed by a highly conserved seven-residue segment DXNDNXP that provides oxygen atoms from both backbone and side-chain carbonyls to chelate the calcium ions that bind at the interface between the domains.[6] We designated these seven-residue segments as "Linkers." Thus, Linker 1 connects Domain 1 to Domain 2, and Linker 2 connects Domain 2 to Domain 3. This is represented schematically in Figure 1(A and C). The amino acid sequence is shown in Figure 1(B). The linkers and core domain regions are highlighted as distinct segments, but they occur within the contiguous amino acid sequence of a single epithelial cadherin molecule. Thus, addition of the linker segments couches Domain 2 in a context that is closer to its physiological setting.

We report the energetics of folding for Domain 2 of epithelial cadherin with no linkers, ECAD2; with the first linker only, L1-ECAD2; with the second linker only, ECAD2-L2; and with both of the linkers, L1-ECAD2-L2, using temperature denaturation monitored by CD. These studies were performed in the absence and presence of calcium and with up to 1 *M* NaCl added (in the absence of calcium). In addition, time-dependent proteolysis with α-chymotrypsin was performed in the presence and absence of calcium. This study provides a critical link between studies of individual domains in cadherin and ongoing studies of the multidomain construct, ECAD12.

MATERIALS AND METHODS

Recombinant Plasmid Construction and Cloning

The original ECAD12 clone was provided by Prof. J. Engel (Biozentrum, Basel, Switzerland) in pET-22b vector that coded for residues from 1 to 220 of the native protein from mouse epithelial cells (Domains 1 and 2, and Linkers 1 and 2). Primers for each of the Domain 2 constructs ECAD2, L1-ECAD2, ECAD2-L2, and L1-ECAD2-L2 [Fig. 1(A)] were designed following the protocol specified in the Ek/LIC cloning kit (Novagen). The Ek/LIC kit adds glutathione S-transferase, His_6-Tag, and S-Tag to the N-terminal end of the protein, allowing for consecutive affinity purification steps. The 5′- and 3′- end primers were designed to amplify the region Glu107–Lys212 (ECAD2), from Asp100–Lys212 for L1-ECAD2, Glu107–Pro219 (ECAD2-L2), Asp100 to Pro219 (L1-ECAD2-L2) [Fig. 1(B)]. PCR amplification was conducted with KOD HiFi DNA Polymerase (Novagen) and dNTPs for 25 cycles following the protocol for KOD HiFi DNA Polymerase. The PCR products were purified using a standard Plasmid Prep Kit (Qiagen). The purified PCR products were treated with T4 DNA Polymerase in the presence of dATP to create 5′ overhang sequences. The treated PCR products were annealed to the pET-41 Ek/LIC vector at the Ek/LIC cloning site located immediately after the N-terminal tags. Competent BL21(DE3)pLysS cells were transformed with

the annealing mix and plated on LB agar plates containing 30 μg/mL kanamycin. Colonies were screened for expression of proteins of the correct molecular weight (SDS-PAGE). The vectors from those colonies were purified and sequenced from the 5′ end of the gene using a primer complementary to the S-tag sequence.

Overexpression and Purification

The four constructs were overexpressed using the BL21(DE3)pLysS expression cell line in 1-L volumes each inoculated with 5 mL overnight culture with 30 μg/mL kanamycin. Cultures (1 L) were grown at 37°C to OD_{600} of ~1, followed by induction with 0.4 m*M* IPTG. At 1.5 h postinduction, the cells were harvested by centrifugation and frozen at −20°C. Pellets from 1 L of culture were resuspended in 10–20 mL of TE buffer, pH 7.4, then lysed using a French pressure cell. After centrifugation, each of the Domain 2 constructs was found in the soluble fraction as indicated in SDS-PAGE.

Each construct was purified in multiple steps and in the same way. The soluble fractions were dialyzed against 20 m*M* Tris/HCl, 0.5 *M* NaCl, 5 m*M* imidazole, pH 7.9, using 10,000 MWCO dialysis membranes (Spectra/Por). The first round of chromatography was conducted on a HiTrap His-Tag column (Amersham) equilibrated with the buffer above. The protein was loaded onto the column then washed with 8 column volumes of the equilibration buffer, and then subsequently with 6 column volumes of 20 m*M* Tris/HCl, 0.5 *M* NaCl, 40 m*M* imidazole, pH 7.9. The protein was eluted with 10 mM Tris/HCl, 250 m*M* NaCl, 0.5 *M* imidazole, pH 7.9, in a step gradient. The fractions from the His-Tag column containing protein were loaded onto a GSTrap column (Amersham) equilibrated with PBS Buffer (20 m*M* potassium phosphate, 0.15 *M* NaCl, pH 7.3). The fractions were eluted with freshly prepared 50 m*M* Tris/HCl, 10 m*M* reducing glutathione, pH 8.0, in a step gradient. Purity of each protein was judged by overloaded Coomassie stained 15% Tris-Glycine SDS-PAGE. Each protein was then dialyzed against 2 m*M* HEPES, 140 m*M* NaCl, pH 7.4. An estimation of protein concentration was made using a BCA assay (Pierce). Each protein was then incubated with light-chain enteropeptidase/enterokinase (0.5 U/mg protein; Prospec) at 37°C for 12–16 h to remove the N-terminal tags. The N-terminal tags and enterokinase were separated from the proteins using SEC on Sephacryl S-100 (1 cm i.d. × 40 cm) equilibrated with 2 m*M* HEPES, 140 m*M* NaCl, pH 7.4. Atomic absorption spectroscopy revealed the level of contaminating calcium in the SEC buffers to be approximately 5 μ*M*. Separation from higher molecular weight components and purity was judged by Coomassie stained overloaded 15% Tris-Glycine SDS-PAGE.

Characterization

The molecular weights of constructs were confirmed by mass spectrometry (MALDI-TOF; University of Iowa, Molecular Analysis Facility). A UV-vis spectrum of each purified protein was taken on a Cary 50 Bio UV-vis spectrophotometer and was typical for proteins with tyrosine (none of the constructs contained tryptophan). The concentration for each protein was obtained using the molar absorptivity 5580 M^{-1} cm^{-1} at 278 nm and a path length of 2 mm. CD spectra for each construct were acquired on a Model 202SF CD Spectrometer (Aviv) from 200 to 300 nm, with a 5 s averaging time in 2 m*M* HEPES, 140 m*M* NaCl, pH 7.4, with no addition (~5 μ*M* contaminating calcium) and in the presence of 5 m*M* Ca^{2+} with a bandwidth of 1 nm. Spectra for each construct were typical for β-sheet protein (data not shown). There was little difference in the spectra upon addition of calcium or salt.

Temperature-Induced Unfolding Studies as a Function of Calcium and Salt

For all temperature-induced unfolding experiments, the 1-cm quartz cuvette was fitted with a screw top to prevent evaporation of the solution at high temperatures. The temperature probe was inserted through the cuvette screw top, and the sample was stirred during data collection. Protein concentrations of 5 or 10 μ*M* in 2 m*M* HEPES, 140 m*M* NaCl, pH 7.4, were used for denaturation experiments. Additional salt-dependent denaturation experiments were performed in 10 m*M* sodium phosphate and 10 μ*M* EGTA, pH 7.4. Added salt (NaCl) concentrations were varied from 0 *M* to 1 *M*. All unfolding measurements spanned a temperature range of 15–85°C. The temperature ramp was set at 1°C/min, with data taken every degree. The equilibration time at each temperature was 30 s. The acquisition time was 5 s. The measurements were taken at 225 nm to increase the signal-to-noise ratio.

The conditions for the calcium-dependent experiments are as follows. Analysis of samples with added 10 μ*M* EGTA yielded identical parameters to samples with no addition of EGTA. This indicates that the low level of contaminating calcium did not impact the energetics of these domains. Calcium-dependent studies were done in two ways. Apo-samples (with no addition of EGTA) were subjected to temperature denaturation and were cooled back to 15°C. Calcium was added to the same solution to a final concentration of 5 m*M* and the protein was again denatured. In a second set of calcium-dependent experiments, high calcium solutions were prepared fresh. Both sets of experiments in 5 m*M* calcium yielded the same results. This concentration of calcium was chosen as two to five times the calcium concentration in the extracellular space.[17,18] Wavelength scans of each protein and buffer were made before and after each unfolding experiment at a temperature of 25°C. Scans before and after the temperature denaturation differed by up to 5%. Parameters reported in tables result from simultaneous analysis of four to six independent data sets.

Data Analysis

All data were analyzed using IGOR Pro (ver.4.0; Wavemetrics) with procedure files written in-house. All data were analyzed according to a two-state unfolding model as governed by the equilibrium constant K_{obs} given in Eq. (1) for which [*U*] is the concentration of the unfolded state and [*N*] is the concentration of the native state at any point along the unfolding profile:

$$K_{obs} = \frac{[U]}{[N]} = e^{-\Delta G_{obs}/RT}. \quad (1)$$

The mole fraction of unfolded species in a solution is given by Eq. (2) for which X_u is the mole fraction of the unfolded species:

$$X_u = \frac{K_{obs}}{1 + K_{obs}}. \quad (2)$$

The relationship between temperature and K_{obs} is given by the Gibbs–Helmholz equation shown below:

$$\Delta G_{obs} = \Delta H_m\left(1 - \frac{T}{T_m}\right) + \Delta C_p\left(T - T_m - T\ln\frac{T}{T_m}\right), \quad (3)$$

where $\Delta G_{obs} = -RT\ln K_{obs}$, ΔH_m is the enthalpy of unfolding at the melting temperature, T_m is the melting temperature, and ΔC_p is the heat capacity at the melting temperature. In fits of data to the model above, ΔC_p could not be resolved independently. This parameter was fixed to 1 kcal/Kmol, a value determined experimentally for ECAD2 in a separate study.[15] Resolved values of ΔH_m and T_m and calculated values for ΔG_{obs} at 25°C (denoted ΔG^0_{un} are reported. With ΔC_p fixed to 0 and 2 kcal/Kmol, resolved parameters differed from those reported by less than 0.1°C in T_m and ~1 kcal/mol in ΔH_m (data not shown). Values for enthalpy (ΔH_{50}) and entropy (ΔS_{50}) at 50°C are reported to facilitate comparison between the constructs.

Proteolytic Susceptibility Studies

The calcium-dependent susceptibility to proteolysis by α-chymotrypsin was tested for samples of each construct (12 μ*M* protein; 0.51 U/mL chymotrypsin) with apo-conditions or 5 m*M* calcium added. Proteins were exposed to protease for 0, 5, 10, 20, 35, and 60 min at room temperature (24°C). Reactions were quenched by addition of 4× SDS-reducing loading buffer and placed in boiling water for 3 min. Proteolyzed samples and an uncleaved control with no protease were screened by SDS-PAGE on 17% Tris-Tricine gels[19] and stained with Coomassie. Bands corresponding to full-length constructs were quantitated in destained gels using Quantity One software supplied with the Gel Doc system (BioRad). The fraction of protein remaining at each time point was calculated by dividing the OD of the full length construct remaining in the digested samples by the OD of the uncleaved control. Error in the quantitation of the individual bands was assumed to be 10% of the OD value for that band. These error values were propagated to yield the errors on the values for "fraction remaining." The calcium-dependence of the protease activity was determined using the chromophoric substrate BTEE (Sigma Chemical Co.). The activity of α-chymotrypsin increased by ~15% with an increase in calcium concentration of four orders of magnitude (1 μ*M* to 10 m*M*). This extends the range of calcium concentration by two orders of magnitude over that tested by Shea et al.[20] to a calcium concentration range in which we observed some calcium-dependent activity.

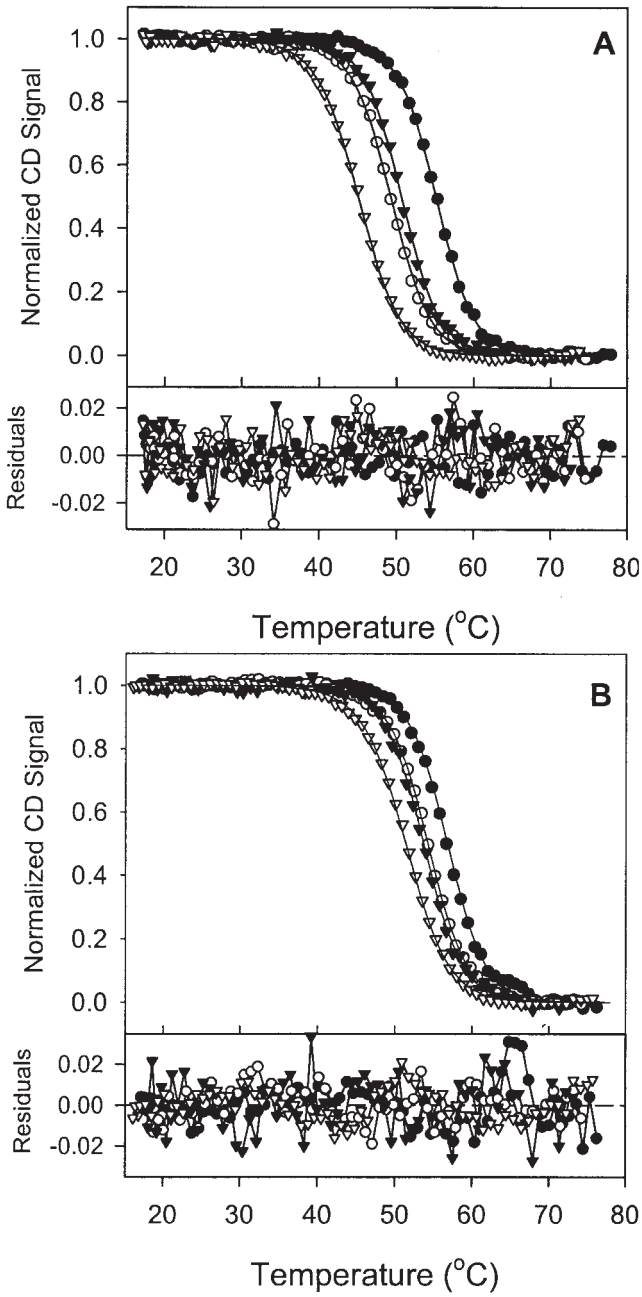

Fig. 2. Temperature denaturation of ECAD2 (●), L1-ECAD2 (○) and ECAD2-L2 (▼) and L1-ECAD2-L2 (▽) at 225 nm, 5 s averaging time with either (**A**) apo-conditions or (**B**) with 5 m*M* calcium added. Normalized CD signal is plotted versus the probe temperature. The dashed lines are simulated based on the parameters resolved from fits to Eqs. (2) and (3) with ΔC_p fixed to 1 kcal/Kmol.

RESULTS

Temperature Denaturation Using Circular Dichroism

Calcium-dependent studies

Figure 2(A) shows the normalized CD signal obtained by temperature denaturation from 15-80°C for each protein in apo-conditions. Solid lines are simulated based on simultaneous fits to all data taken under those conditions.

TABLE I. Resolved Thermodynamic Parameters for ECAD2 With the Adjacent Linkers[a]

	Apo		5 m*M* Ca^{2+}			
Construct	T_m (°C)	[b]ΔG^0_{un} (kcal/mol)	T_m (°C)	[b]ΔG^0_{un} (kcal/mol)	[c]ΔT_m (°C)	[c]ΔG^0_{un} (kcal/mol)
ECAD2	54.7 ± 0.6	6.3 ± 0.2	56.8 ± 0.1	6.7 ± 0.1	2.1 ± 0.6	0.4 ± 0.2
L1-ECAD2	49.2 ± 0.1	5.1 ± 0.1	54.2 ± 0.1	6.1 ± 0.1	5.0 ± 0.1	1.0 ± 0.1
ECAD2-L2	50.6 ± 0.1	5.6 ± 0.1	53.7 ± 0.1	6.0 ± 0.1	3.1 ± 0.1	0.4 ± 0.1
L1-ECAD2-L2	45.1 ± 0.4	3.9 ± 0.1	51.4 ± 0.1	4.9 ± 0.1	6.3 ± 0.4	1.0 ± 0.1

[a]Melting temperature (T_m) result from fits with ΔC_p fixed to 1 kcal/Kmol.
[b]Calculated using Eq. (3) at 25°C.
[c]Difference between 5 m*M* calcium and apo-parameters.

Upon inspection of the data, Domain 2 without either linker was most stable. Addition of one linker on either terminus destabilized the protein by ~5°C. Addition of both linkers destabilized the domain by ~10°C. Figure 2(B) shows the normalized CD signal from temperature denaturation for each protein in high calcium concentration (5 m*M*). The addition of calcium caused the denaturation profiles to shift to higher temperature and cluster at a position closer to that observed for ECAD2.

Table I contains the stability at 25°C and melting temperature (T_m) for Domain 2, with and without linker regions in low and high calcium resolved from analysis of the data shown in Figure 2(A and B). At low calcium concentrations the T_m values were in the relative order of ECAD2 > ECAD2-L2 ≈ L1-ECAD2 > L1-ECAD2-L2. ΔG^0_{un} values tracked the T_m values. These data can be summarized as follows. Linker 1 showed a more destabilizing effect on ECAD2 than did Linker 2; $\Delta\Delta G^0_{un}$ [ECAD2 to L1-ECAD2] = −1.2 ± 0.2 kcal/mol; $\Delta\Delta G^0_{un}$ [ECAD2 to ECAD2-L2] = −0.7 ± 0.2 kcal/mol. The addition of both linker regions reduced the stability by slightly greater than the sum of the two individual effects $\Delta\Delta G^0_{un}$ [ECAD2 to L1-ECAD2-L2] = −2.4 ± 0.2 kcal/mol (see Table II). Thus, in low calcium concentrations, the contribution of each linker to the destabilization of Domain 2 was roughly additive.

In the presence of 5 m*M* calcium, we resolved values for ΔH_m that were unchanged from the apo samples (data not shown). T_m values were significantly shifted upon addition of calcium, indicating that calcium stabilized these constructs (see ΔT_m in Table I). There was greater calcium stabilization in L1-ECAD2 than in ECAD2-L2. The calcium-dependent shift in T_m for L1-ECAD2-L2 was less than the sum of the shifts for either linker alone. The value of ΔG^0_{un} was increased for all constructs with linkers upon addition of calcium (see $\Delta\Delta G^0_{un}$ in Table I). The increase was not as great for ECAD2 and ECAD2-L2, indicating that there is less calcium stabilization in these two constructs. Constructs containing Linker 1 (L1-ECAD2 and L1-ECAD2-L2) showed the largest calcium-dependent increase in stability.

The calcium-dependent shift in ΔG^0_{un} can be used to estimate an apparent calcium-binding constant for one ligand to the Linker 1–Domain 2 interface according to the equation

$$\Delta G_b = -RT \ln(1 + K_b[Ca^{2+}]) \quad (4)$$

TABLE II. Effect of Additional Segments on Melting Temperature and Stability[a]

Protein	No. of res.	ΔT_m (°C)	$\Delta\Delta G_{un}{}^0$ (kcal/mol)
Ab1[b]	4	7.5	1.19
Ab1[b]	11	8.2	1.19
M11[b]	6	15.9	4.31
Ferricytochrome b_5[c]	6	5.8	3.79
Ferrocytochrome b_5[c]	6	6.2	5.07
TNfn31-90[d]	2	7.3 ± 0.1	2.37 ± 0.21
M5[e]	6	15.9	NA
N-domain calmodulin[f]	5	9	1.05
ΔN-H2A/H2B[g]	31	NA	−0.7 ± 0.1
H2A/ΔN-H2B[g]	15	NA	0.4 ± 0.1
WT-H2A/H2B[g]	15 ± 31	NA	0.0 ± 0.3
L1-ECAD2[h]	7	−5.5 ± 0.1	−1.2 ± 0.2
ECAD2-L2[h]	7	−4.1 ± 0.1	−0.7 ± 0.2
L1-ECAD2-L2[h]	14	−9.6 ± 0.1	−2.4 ± 0.2

[a]All values are reported as they were in the original manuscript.
[b]Modular domain (100 residues) from titin of human cardiac muscle. Construct contains an N-terminal His_6 plus two serines.[21]
[c]Tryptic fragment of microsomal cytochrome b5 (≈100 residues).[22]
[d]Fibronectin type III domain with residues added at the C-terminus from Tenascin in the apo-state.[23]
[e]Same notes as footnote b.[24]
[f]N-terminal domain of *Paramecium* calmodulin.[25,26]
[g]Stability of histone H2A/H2B dimer with (WT-) or without (ΔN-) the N-terminal tails. These data are relative to the stability of the ΔN-H2A/ΔN-H2B construct (both N-terminal tails missing).[27]
[h]Constructs reported in this article relative to ECAD2 (107–212) in low calcium.
NA, data was not available.

where ΔG_b is the binding free energy change at the calcium concentration [Ca^{2+}] and K_b is the binding constant for calcium.[28] In this case, ΔG_b was 1.0 kcal/mol, and [Ca^{2+}] was 5 m*M*, yielding a binding constant of ~1000 M^{-1}. This calculation assumes a stoichiometric of one.

In order to assess the relative contributions of enthalpy and entropy to the unfolding process, these parameters were calculated at a common temperature (50°C) as reported in Table III. The enthalpy was similar for ECAD2, L1-ECAD2, and ECAD2-L2, but significantly less for L1-ECAD2-L2 regardless of the calcium level. Entropy values at 50°C are reported, as well as the entropy values corrected for the number of residues in the construct. The entropy per residue value decreased upon the addition of both linkers in the absence and presence of calcium.

TABLE III. Comparison of Enthalpy and Entropy Values at a Common Temperature[a]

	Apo			5 m*M* Ca^{2+}		
Construct	ΔH_{50} (kcal/mol)	ΔS_{50} (cal/kmol)	$\Delta S_{50/res}$ (cal/Kresidue)	ΔH_{50} (kcal/mol)	ΔS_{50} (cal/Kmol)	$\Delta S_{50/res}$ (cal/Kresidue)
ECAD2	80.6 ± 1.6	246 ± 5	2.3	79.5 ± 1.4	241 ± 4	2.3
L1-ECAD2	81.1 ± 1.1	252 ± 3	2.2	79.3 ± 1.2	242 ± 4	2.1
ECAD2-L2	83.3 ± 1.1	257 ± 3	2.3	79.4 ± 1.1	243 ± 3	2.1
L1-ECAD2-L2	76.9 ± 2.5	242 ± 8	2.0	73.0 ± 0.9	225 ± 3	1.9

[a]Enthalpy (ΔH_{50}) and entropy (ΔS_{50}) at 50°C calculated from resolved values of T_m and ΔH_m from fits with ΔC_p fixed to 1 kcal/Kmol.

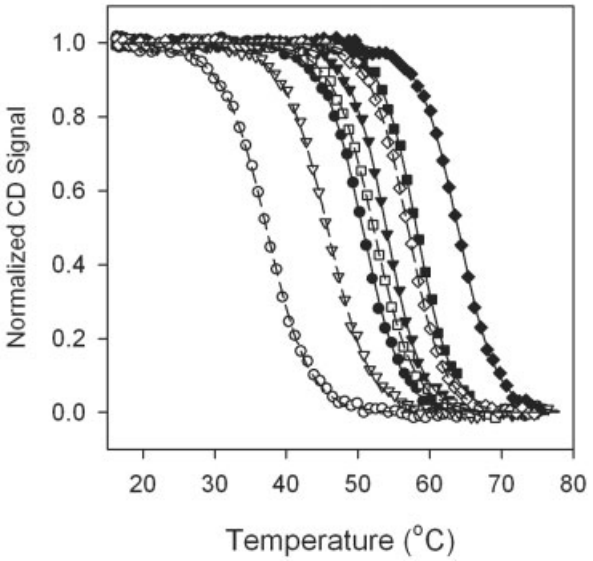

Fig. 3. Normalized CD data from the temperature denaturation of ECAD2 (solid symbols) and L1-ECAD2-L2 (open symbols) at 0 *M* (circles), 140 m*M* (triangles), 500 m*M* (squares), and 1 *M* (diamonds) NaCl added to solutions buffered with 10 m*M* sodium phosphate, 10 μ*M* EGTA at pH 7.4. Lines through data were simulated based on the best fit values for ΔH_m and T_m resolved from fits to Eq. (3). ΔC_p was fixed to 1 kcal/Kmol.

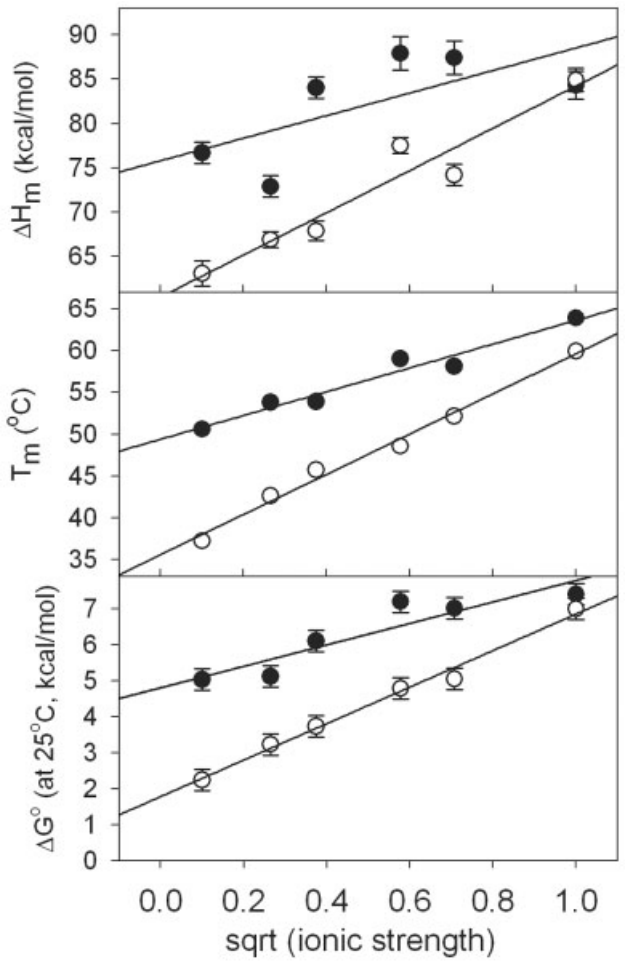

Fig. 4. Thermodynamic parameters resolved from analysis of temperature-denaturation studies as a function of ionic strength of the buffer. (**A**) Enthalpy at the melting temperature, (**B**) the melting temperature, and (**C**) the free energy change for unfolding calculated from ΔH_m and T_m values are shown for ECAD2 (solid symbols) and L1-ECAD2-L2 (open symbols). Solid lines are linear fits to the data.

Salt-dependent studies

Figure 3 shows the normalized CD signal obtained by temperature denaturation for constructs ECAD2 and L1-ECAD2-L2 at four salt concentrations. These are a subset of the experiments that were done. The transitions for both the constructs moved to higher temperature with the increase in salt concentration. This effect was enhanced for L1-ECAD2-L2 (T_m span was ~20°C) than seen for ECAD2 (T_m span was ~15°C) over the range of added salt from 0 to 1 *M* NaCl. A difference in slope of the transitions was also apparent; that is, the lower salt concentrations yielded shallower transitions.

Results from fits of the melting transitions to Eq. (3) are shown graphically for six different added salt concentrations in Figure 4. For both constructs, ΔH_m, T_m, and ΔG^0_{un} increased with the square root of the ionic strength (0 to 1 *M* added NaCl). The maximum difference for both constructs was at 0 *M* added salt, and the minimum difference was at 1 *M* added salt for all three parameters. The parameters for ECAD2 appeared to plateau between 200 and 400 m*M* added NaCl. Those for L1-ECAD2-L2 continued to rise to 1 *M* added NaCl. A subset of these experiments performed on the L1-ECAD2 and ECAD2-L2 constructs displayed a similar trend.

Values for ΔH_{50} and ΔS_{50} were determined as a function of [NaCl] (data not shown). There was no salt-dependent trend in these data. The average values for $T\Delta S_{50}$ were 74.1 ± 5.0 (ECAD2) and 76.2 ± 3.5 (L1-ECAD2-L2) kcal/mol. The average values for ΔH_{50} were 75.6 ± 4.8 (ECAD2) and 75.7 ± 2.5 (L1-ECAD2-L2) kcal/mol.

It is also interesting to note that studies on L1-ECAD2-L2 at 3 *M* added NaCl showed enthalpies and free energies of unfolding that were twice those at 1 *M* NaCl (data not shown). It is likely that this domain forms dimers under extremely high salt conditions. Kirchoff plots of the salt-dependent data yielded estimates of ΔC_p of 0.8 ± 0.5 kcal/Kmol (less well determined) for ECAD2 and 0.97 ± 0.16 kcal/Kmol for L1-ECAD2-L2 (data not shown). These are consistent with using the value 1 kcal/Kmol in the analysis of data.

Proteolytic susceptibility studies

Figure 5(A) shows example SDS-PAGE data that were analyzed to create the fractional susceptibility shown in Figure 5(B). The "start" band in each gel was clearly in the highest abundance. The small decrease in the abundance of the full-sized protein band at the 0 min time point indicated the amount of proteolysis that occurred before the reaction was quenched. In the presence of calcium [bottom panel in Fig. 5(A)], there was less proteolysis at each time point than in the absence of calcium [upper panel in Fig. 5(A)]. The full-sized protein band in the lower panel is denser than the band in the upper panel at each time point. There were no significant cleavage products apparent in the gels for any construct indicating complete digestion of the proteins once the primary cut was made. The top panel in Figure 5(B) shows the decrease in the abundance of the full-length construct in low calcium as a function of digest time. All four constructs were proteolyzed at the same rate in low calcium concentration regardless of whether or not linker segments were present. The similarity in susceptibility in the absence of calcium is consistent with the primary cleavage occurring at Y142, the only aromatic residue not located within a region of the β-sheet hydrogen bonding network [see Fig. 1(B) and Table IV].

The lower panel in Figure 5(B) shows the decrease in the abundance of full-length construct at 5 m*M* calcium as a function of digest time. Constructs with Linker 1 (L1-ECAD2 and L1-ECAD2-L2) showed a reduced susceptibility in the presence of calcium. The susceptibility of ECAD2-L2 was independent of the calcium concentration. ECAD2 showed a marked increase in susceptibility upon addition of calcium.

DISCUSSION

In this article, we report the creation of four constructs that systematically test the effect of adjoining linker regions upon the energetic profile for stability of Domain 2 of epithelial cadherin. Earlier studies on ECAD2 employed complementary techniques that yielded very similar thermodynamic parameters that govern the stability of Domain 2.[15] Based on those studies, we are confident that temperature–denaturation monitored by CD reported here gives an accurate representation of the thermodynamics of protein stability in the ECAD2 constructs with the adjacent linkers attached.

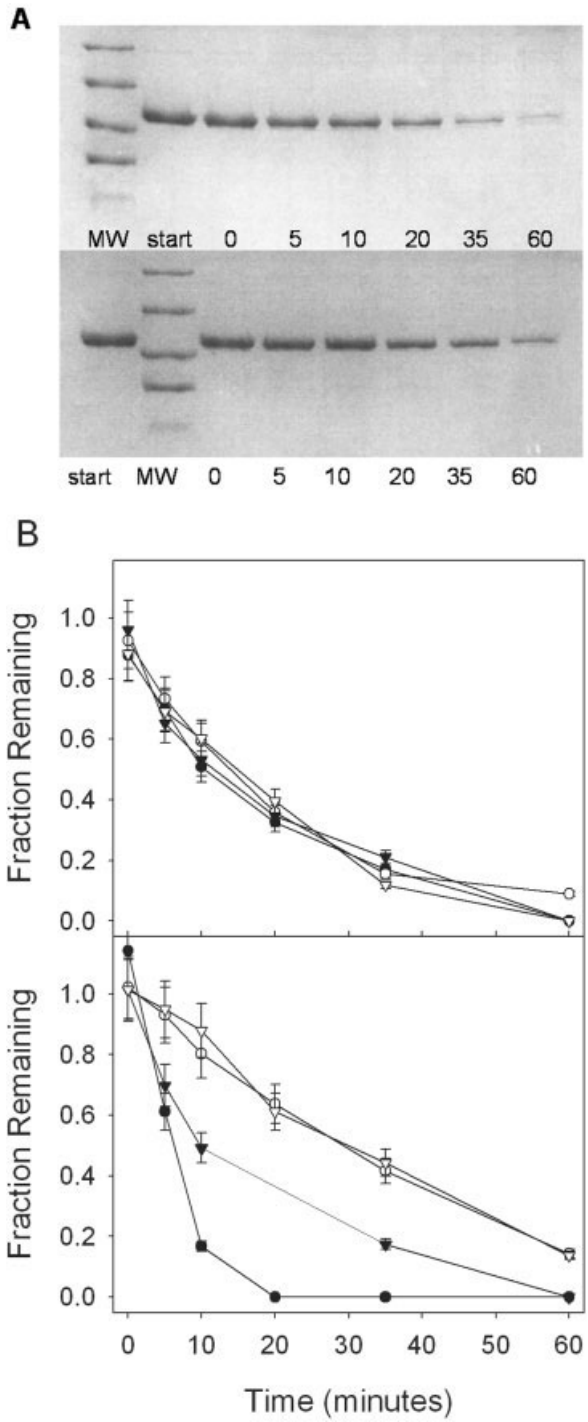

Fig. 5. Proteolytic susceptibility. (**A**) Coomassie-stained, Tris-Tricine gels (17%) of time-dependent digests of L1-ECAD2-L2. The top gel is in apo-conditions. The bottom gel is in 5 m*M* calcium. Digest time (min) is noted below each lane (~1.4 μg/lane). Molecular weight markers (MW) range from 26.6 to 3.5 kD. The lane marked "start" is the uncleaved control. (**B**) The fraction of full-length protein remaining in apo-conditions (top plot) and in high calcium (5 m*M*; bottom plot) for each construct ECAD2 (●), L1-ECAD2 (○) and ECAD2-L2 (▼) and L1-ECAD2-L2 (▽) are plotted at 0, 5, 10, 20, 35, and 60 min of exposure to α-chymotrypsin.-

TABLE IV. Accessible Surface Area of Acidic, Basic, and Aromatic Residues in L1-ECAD2-L2[a]

Acidic		Basic		Aromatic	
Residue	% ASA	Residue	% ASA	Residue	% ASA
D100	18.0	R105	70.9	F108	2.8
D103	69.0	K129	65.6	F113	5.3
E107	85.6	K160	70.6	Y142	73.9
E111	100.0	R167	57.8	Y148	7.7
E114	84.3	R181	42.9	F163	0.2
E119	34.5	K206	58.7	Y187	0.0
D134	1.1	K212	61.7		
D136	1.3				
D137	25.6				
D138	67.8				
D154	81.5				
E156	55.4				
D168	80.8				
D180	44.2				
E182	90.4				
D195	0.0				
D199	81.5				
D213	88.2				
D216	NA				

[a]Areas were calculated by GET AREA (v. 1.1; available at www.scsb.utmb.edu/cgi-bin/get_a_form.tc1.[24]
Based on structure by Nagar et al.[6] Calcium atoms were removed, but structure was not reminimized. NA, indicates that the residue was not ordered in the crystal structure.

Destabilization of Domain 2 by Adjoining Linker Segments

One of the most interesting findings reported in this work is that ECAD2 is destabilized by the addition of the adjoining segments of seven amino acids. These segments were added piecewise to the N-terminus and C-terminus of Domain 2 and comprise the sequences bordering Domain 2 as part of a five-domain series. We believe that the destabilizing effect of the linker segments is due to their anionic nature.

Salt dependence of stability

Based on the exposure of acidic residues, we hypothesize that electrostatic repulsion contributes to the destabilization effect. We report here initial studies of the effect of NaCl upon the stability of these constructs. Salt-dependence studies were performed under apo-conditions, since the primary destabilization effect from the linkers was observed in the absence of calcium. Salt stabilized the constructs significantly (see Figs. 3 and 4). This is consistent with repulsive electrostatic interactions that are effectively screened in NaCl solutions.[30–32] It is not clear from these limited studies whether this is specific binding by Na^+ or a simple screening effect. Stabilization of ECAD2 by salt indicates that there was significant electrostatic repulsion on the surface of the core domain even in the absence of linkers. Salt had a greater effect on L1-ECAD2-L2, consistent with an increased effect due to electrostatic repulsion from both of the linkers. At 1 *M* NaCl, ECAD2 and L1-ECAD2-L2 have relatively similar energetic profiles indicating that the destabilizing effect of the linkers is reduced in high salt (Fig. 4).

Close inspection of the structural features of Domain 2 constructs revealed interesting information that supports the repulsion explanation for the destabilizing effect of linkers. Domain 2 constructs are acidic proteins with pI's ranging from 4.4 to 4.5 (SEDNTERP; J. Philo). Many of the charged residues are exposed on the surface of the protein. Table IV shows the acidic residues in L1-ECAD2-L2 that are ordered in the crystal structure by Nagar et al.[6] Of the 18 structured acidic amino acid residues, 11 have at least 50% of their surface area accessible to a 1.4 Å probe. Note that D134, D136, and D195 are buried with their charged moieties inaccessible to solvent. This is due to their role in chelating calcium in the structure that is inaccessible to a solvent probe of the surface. It is likely that these loop regions restructure in the absence of calcium, thereby increasing their accessible surface area. Seven of the eight basic residues are at least 50% exposed on the surface of the protein. Thus, there is predominance of acidic residues exposed on the surface of the protein.

Entropy and enthalpy considerations

Entropy and enthalpy of unfolding at a fixed temperature (50°C) was similar for ECAD2, L1-ECAD2, and ECAD2-L2 in both calcium levels. Both entropy and enthalpy decreased for the construct with both linkers (L1-ECAD2-L2). Addition of 5 m*M* calcium did not restore the values for L1-ECAD2-L2 to those found for the apo condition of ECAD2. Overall, these differences in entropy and enthalpy are small and do not show a sufficiently systematic trend to argue the observed change in T_m.

The value for ΔS_{50} was corrected for the number of residues in each construct in order to normalize for the effect of the length upon the conformational entropy of the unfolded state. Assuming that the unfolded state for each construct is equivalent, the low corrected entropy value ($\Delta S_{50/res}$) for L1-ECAD2-L2 reflects the greater entropy of the folded state.[33–35] Thus, the lower entropy and lower enthalpy are both consistent with the lower stability of L1-ECAD2-L2.

Comparison to similar domains in the literature

The observed destabilization from additional sequences reported here is in contrast to a number of similar studies of diverse domains. Table II contains data from the literature for domains whose stability has been studied in the absence and presence of short additions of amino acids at either the N- or C-terminus. The majority of these proteins have similar folds to the protein under study here. In each of these cases except for one, peptide additions led to stabilization of the domains as manifested by an increase in T_m and ΔG^0_{un} .

One of the examples from the literature shown in Table II is particularly relevant to our studies. Placek and Gloss[27] reported that the stability of the histone 2 dimer (WT-H2A/H2B) is affected by the presence of the highly basic N-terminal tails. These tails have weak electron density in the crystal structure of the nucleosome core particle[36] and

are thought to be involved in interactions between neighboring nucleosomes. The data of Placek and Gloss is summarized in Table II relative to the histone 2 dimer with both N-terminal tails removed (ΔN-H2A/ΔN-H2B). The dimer is destabilized when the N-terminal tail of H2B is present. This is an analogous situation to our observations with the addition of the linker regions. Conversely, the H2A/H2B dimer is stabilized when the N-terminal tail of H2A is present.

Reports vary in the literature regarding the effect on stability due to interactions between immunoglobulin-type domains. In a similar fashion to our observations for Domain 2 of cadherin, Wenk et al. reported that the isolated N-terminal domain of Protein S is slightly more stable when isolated from the C-terminal domain than in the intact protein ($\Delta T_m = 5$°C).[37] More typically, however, in this same protein, the C-terminal domain is significantly stabilized in the intact protein. Stabilization due to interdomain interactions has also been observed for the $X1_1$ domain of cellobiohydrolase.[38] This domain is a fibronectin type III domain of 170 amino acids residues that is stabilized by 6.4°C by the presence of it neighboring domain, $X1_2$.

Stability parameters of our constructs are also comparable to other modular proteins with similar immunoglobulinlike folds. Modular domain I28 (100 residues) of titin from human cardiac muscle[39] and twitchin Ig 18′, a modular domain from muscle protein of a nematode,[40] at neutral pH had T_m values of ~54°C, similar to that of our constructs. However, their ΔG^0_{un} values were ~2 kcal/mol smaller than our constructs. This is likely due to the relatively high value of ΔH_m for ECAD2.[15] Contrary to the studies reported here, studies of titin module I27 showed an ionic strength dependent decrease in stability.[39] Another example is CD2 antigen from rat T-lymphocyte that had a very similar ΔG^0_{un} value (6.35 kcal/mol) to that of ECAD2 at neutral pH, but is likely due to its higher T_m value of ~64°C.[39] In these examples, the proteins were denatured using guanidine HCl at neutral pH.

Calcium Binding to Domain 2 Constructs

Although we do not know the stoichiometry, there are two lines of evidence that calcium binds to the constructs with linkers. First, there is a calcium-induced decrease in susceptibility to proteolysis by α-chymotrypsin upon addition of calcium, particularly for the two constructs containing Linker 1. This likely results from occluding of the primary cleavage site at Y142 (see Table IV) due to binding of calcium at the Domain 2–Linker 1 interface. Note that all phenylalanines and tyrosines are less that 10% accessible except for Y142, which is 75% accessible (Table IV). This is consistent with this residue as the primary cleavage site for α-chymotrypsin. Second, there is distinct calcium-induced stabilization observed for each construct with Linker 1 in the temperature-induced denaturation profiles and in the resolved values for T_m. An apparent calcium binding constant was calculated in the Results section. This is a single-point determination of the binding constant of the constructs containing Linker 1 based on the linkage between binding and stability. In spite of this limitation, the binding constants estimated here were on the order of those for the low affinity ligand predicted by Koch et al for the two-domain construct.[41] Similar binding affinities were resolved in studies of calcium[42] and cadmium[43] binding to a synthetic peptide containing an important loop in Domain 2. These values are also similar to values for calcium binding to synthetic peptides that include the linker region.[44]

Figure 1(B) shows the amino acid sequence of L1-ECAD2-L2 with the putative residues involved in binding calcium. Those residues that are involved in binding calcium at the interface between Domains 1 and 2 were apparent in the crystal structure of the two-domain construct by Nagar et al.[6] Although three calciums were present in the structure, only one used oxygens from Linker 1 and Domain 2 only (Ca3 in Nagar et al.). In particular, side-chain oxygens are involved from residues D134, D136, and N143 in the loop connecting the b- and c-strands. D195 in the loop connecting the e- and f-strands is also involved, as well as the side-chain carbonyl from N102 and the backbone carbonyl from N104 in Linker 1. As one would expect, all of these residues are in the loops that connect the strands that are "up" in the schematic in Figure 1(C). Thus, it is possible that these residues are involved in the association of calcium to Domain 2 constructs containing Linker 1.

Calculated values for ΔG^0_{un} show small, but significant stabilization for the ECAD2 and ECAD2-L2 constructs. Based on analogous positions in Domain 1 from the crystal structure [residues are marked in Fig. 1(B)], we inferred that residues E119, D180, E182, and D216 are important for ligand binding in the Domain 2–Domain 3 interface region [Fig. 1(C)]. These may be involved in the association of calcium to constructs containing Domain 2 and Linker 2 (ECAD2-L2 and L1-ECAD2-L2). However, this association was weaker than ions at the Domain 2–Linker 1 interface. This apparent association with the Domain 2–Linker 2 interface is similar to the ion association with neural cadherin in the crystal structure by Shapiro et al.[45] In this structure of Domain 1–Linker 1 of neural cadherin, ions (UO_2^{2+} and Yb^{3+}) associated at the same positions as the calcium ions in the crystal structure of the two-domain construct of epithelial cadherin.[6] This indicates that ions can associate at the "bottom" of a domain in the presence of the following linker.

Calcium-binding proteins that undergo conformational change upon binding calcium may exhibit this as endo- or exothermic processes. For example, cation binding to SynCaM (EF-hand protein) was endothermic,[46] while binding to oxidized SynCaM was exothermic.[47] The constructs under study here did not display significant calcium-dependent change in the value of ΔH_m. This may indicate that there was little conformational change upon calcium binding in our constructs.

Several observations can be made regarding the data presented here and studies in the literature. First, since the majority of the acidic residues have greater than 50% accessible surface area, one would expect them to be

charged with pKa values near their canonical values.[48] Second, it is likely that binding of calcium is specific, since Ca^{2+} is the ion that associates at the domain interfaces in nature. Sodium provided a poor substitute for calcium in that addition of 5 m*M* Ca^{2+} was equivalent energetically to addition of 400 m*M* Na^{+}. Third, the salt-dependent increase in stability is similar in magnitude to that seen for the acidic, multimeric, halophilic protein malate dehydrogenase from *Haloarcula marismortui*[49] and somewhat larger than that observed for apoflavodoxin.[31] Finally, H2A/H2B dimer from the nucleosome core particle exhibited a NaCl-dependent increase in stability that was attributed to a role for electrostatic repulsion in destabilizing the dimer.[27,50] As mentioned earlier, although H2A/H2B is basic and a dimer, the effect of the relatively unstructured N-terminal tail of H2B on the stability of the core domain is similar to the effect of the linker segments on ECAD2. The salt-dependent studies reported here lay the foundation for more systematic experimental studies of the effect of cations upon stability of the modular domains of cadherin.

In conclusion, we find this study particularly important in that it elucidates an example in which extending the boundaries of a domain by adding seven residues of adjacent sequence significantly destabilized the domain in the absence of calcium. This is in contrast to literature reports for similar domains. Thus, it is the nature rather than the number of residues added that determines the effect upon stability. These studies are a critical link between characterization of an isolated domain and multidomain complex. Second, addition of the linker segments, particularly Linker 1, created an environment for coordination of a calcium ion leading to a greater calcium-induced stabilization. Finally, the salt-induced stabilization of these constructs is consistent with charge–charge repulsion as a contributor to the destabilizing effect of the linkers. The results reported here lay the foundation for more systematic experimental studies of the effect of cations upon stability of the modular domains of cadherin and open up interesting questions regarding the behavior of modular proteins.

REFERENCES

1. Takeichi M. Cadherins: a molecular family important in selective cell–cell adhesion. Annu Rev Biochem 1990;59:237–252.
2. Alattia JR, Kurokawa H, Ikura M. Structural view of cadherin-mediated cell–cell adhesion. Cell Mol Life Sci 1999;55:359–367.
3. Kemler R, Ozawa M, Ringwald M. Calcium-dependent cell adhesion molecules. Curr Opin Cell Biol 1989;1:892–897.
4. Overduin M, Harvey TS, Bagby S, Tong KI, Yau P, Takeichi M, Ikura M. Solution structure of the epithelial cadherin domain responsible for selective cell adhesion. Science 1995;267:386–389.
5. Overduin M, Tong KI, Kay CM, Ikura M. ^{1}H, ^{15}N and ^{13}C resonance assignments and monomeric structure of the amino-terminal extracellular domain of epithelial cadherin. J Biomol NMR 1996;7:173–189.
6. Nagar B, Overduin M, Ikura M, Rini JM. Structural basis of calcium-induced E-cadherin rigidification and dimerization. Nature 1996;380:360–364.
7. Pertz O, Bozic D, Koch AW, Fauser C, Brancaccio A, Engel J. A new crystal structure, Ca^{2+} dependence and mutational analysis reveal molecular details of E-cadherin homoassociation. EMBO J 1999;18:1738–1747.
8. Nose A, Tsuji K, Takeichi M. Localization of specificity determining sites in cadherin cell adhesion molecules. Cell 1990;61:147–155.
9. Amagai M, Karpati S, Prussick R, Klaus-Kovtun V, Stanley JR. Autoantibodies against the amino-terminal cadherin-like binding domain of *Pemphigus vulgaris* antigen are pathogenic. J Clin Invest 1992;90:919–926.
10. Tamura K, Shan WS, Hendrickson WA, Colman DR, Shapiro L. Structure–function analysis of cell adhesion by neural (N-) cadherin. Neuron 1998;20:1153–1163.
11. Shan WS, Koch A, Murray J, Colman DR, Shapiro L. The adhesive binding site of cadherins revisited. Biophys Chem 1999;82:157–163.
12. Boggon TJ, Murray J, Chappuis-Flament S, Wong E, Gumbiner BM, Shapiro L. C-cadherin ectodomain structure and implications for cell adhesion mechanisms. Science 2002;296:1308–1313.
13. Pokutta S, Herrenknecht K, Kemler R, Engel J. Conformational changes of the recombinant extracellular domain of E-cadherin upon calcium binding. Eur J Biochem 1994;223:1019–1026.
14. Takeichi M. Functional correlation between cell adhesive properties and some cell surface proteins. J Cell Biol 1977;75:464–474.
15. Prasad A, Housley NA, Pedigo S. Thermodynamic stability of domain 2 of epithelial cadherin. Biochemistry 2004;43:8055–8066.
16. Tomschy A, Fauser C, Landwehr R, Engel J. Homophilic adhesion of E-cadherin occurs by a co-operative two-step interaction of N-terminal domains. EMBO J 1996;15:3507–3514.
17. Brown EM, Vassilev PM, Hebert SC. Calcium ions as extracellular messengers. Cell 995;83:679–682.
18. Maurer P, Hohenester E, Engel J. Extracellular calcium-binding proteins. Curr Opin Cell Biol 1996;8:609–617.
19. Schagger H, von Jagow G. Tricine-sodium dodecyl sulfate–polyacrylamide gel electrophoresis for the separation of proteins in the range from 1 to 100 kDa. Anal Biochem 1987;166:368–379.
20. Shea MA, Sorenson BR, Pedigo S, Verhoeven AS. Proteolytic footprinting titrations for estimating ligand-binding constants and detecting pathways of conformational switching of calmodulin. Methods Enzymol 2000;323:254–301.
21. Politou AS, Gautel M, Joseph C, Pastore A. Immunoglobulin-type domains of titin are stabilized by amino-terminal extension. FEBS Lett 1994;352:27–31.
22. Newbold RJ, Hewson R, Whitford D. The thermal stability of the tryptic fragment of bovine microsomal cytochrome b5 and a variant containing six additional residues. FEBS Lett 1992;314:419–424.
23. Hamill SJ, Meekhof AE, Clarke J. The effect of boundary selection on the stability and folding of the third fibronectin type III domain from human tenascin. Biochemistry 1998;37:8071–8079.
24. Pfuhl M, Improta S, Politou AS, Pastore A. When a module is also a domain: the role of the N terminus in the stability and the dynamics of immunoglobulin domains from titin. J Mol Biol 1997;265:242–256.
25. Sorensen BR, Faga LA, Hultman R, Shea MA. An interdomain linker increases the thermostability and decreases the calcium affinity of the calmodulin N-domain. Biochemistry 2002;41:15–20.
26. Faga LA, Sorensen BR, VanScyoc WS, Shea MA. Basic interdomain boundary residues in calmodulin decrease calcium affinity of sites I and II by stabilizing helix–helix interactions. Proteins 2003;50:381–391.
27. Placek BJ, Gloss LM. The N-terminal tails of the H2A-H2B histones affect dimer structure and stability. Biochemistry 2002;41:14960–14968.
28. Schellman JA. Macromolecular binding. Biopolymers 1975;14:999–1018.
29. Fraczkiewicz R, Braun W. Exact and efficient calculation of the accessible surface areas and their gradients for macromolecules. J Comp Chem 1998;19:319–333.
30. Garcia-Moreno B. Probing structural and physical basis of protein energetics linked to protons and salt. Methods Enzymol 1995;259:512–538.
31. Maldonado S, Irun MP, Campos LA, Rubio JA, Luquita A, Lostao A, Wang R, Garcia-Moreno EB, Sancho J. Salt-induced stabilization of apoflavodoxin at neutral pH is mediated through cation-specific effects. Protein Sci 2002;11:1260–1273.
32. Record MT Jr, Zhang W, Anderson CF. Analysis of effects of salts and uncharged solutes on protein and nucleic acid equilibria and processes: a practical guide to recognizing and interpreting poly-

electrolyte effects, Hofmeister effects, and osmotic effects of salts. Adv Protein Chem 1998;51:281–353.
33. Privalov PL. Stability of proteins: small globular proteins. Adv Protein Chem 1979;33:167–241.
34. Sturtevant JM. Heat capacity and entropy changes in processes involving proteins. Proc Natl Acad Sci USA 1977;74:2236–2240.
35. Makhatadze GI, Privalov PL. On the entropy of protein folding. Protein Sci 1996;5:507–510.
36. Luger K, Mader AW, Richmond RK, Sargent DF, Richmond TJ. Crystal structure of the nucleosome core particle at 2.8 Å resolution. Nature 1997;389:251–260.
37. Wenk M, Jaenicke R, Mayr EM. Kinetic stabilisation of a modular protein by domain interactions. FEBS Lett 1998;438:127–130.
38. Kataeva IA, Uversky VN, Ljungdahl LG. Calcium and domain interactions contribute to the thermostability of domains of the multimodular cellobiohydrolase, CbhA, a subunit of the *Clostridium thermocellum* cellulosome. Biochem J 2003;372:151–161.
39. Politou AS, Thomas DJ, Pastore A. The folding and stability of titin immunoglobulin-like modules, with implications for the mechanism of elasticity. Biophys J 1995;69:2601–2610.
40. Fong S, Hamill SJ, Proctor M, Freund SM, Benian GM, Chothia C, Bycroft M, Clarke J. Structure and stability of an immunoglobulin superfamily domain from twitchin, a muscle protein of the nematode *Caenorhabditis elegans*. J Mol Biol 1996;264:624–639.
41. Koch AW, Pokutta S, Lustig A, Engel J. Calcium binding and homoassociation of E-cadherin domains. Biochemistry 1997;36: 7697–7705.
42. Ozawa M, Engel J, Kemler R. Single amino acid substitutions in one Ca^{2+} binding site of uvomorulin abolish the adhesive function. Cell 1990;63:1033–1038.
43. Prozialeck WC, Lamar PC. Interaction of cadmium [Cd(2+)] with a 13-residue polypeptide analog of a putative calcium-binding motif of E-cadherin. Biochim Biophys Acta 1999;1451:93–100.
44. Yang W, Tsai T, Kats M, Yang JJ. Peptide analogs from E-cadherin with different calcium-binding affinities. J Pept Res 2000;55:203–215.
45. Shapiro L, Fannon AM, Kwong PD, Thompson A, Lehmann MS, Grubel G, Legrand JF, Als-Nielsen J, Colman DR, Hendrickson WA. Structural basis of cell–cell adhesion by cadherins [see comments]. Nature 1995;374:327–337.
46. Gilli R, Lafitte D, Lopez C, Kilhoffer M, Makarov A, Briand C, Haiech J. Thermodynamic analysis of calcium and magnesium binding to calmodulin. Biochemistry 1998;37:5450–5456.
47. Lafitte D, Tsvetkov PO, Devred F, Toci R, Barras F, Briand C, Makarov AA, Haiech J. Cation binding mode of fully oxidised calmodulin explained by the unfolding of the apostate. Biochim Biophys Acta 2002;1600:105–110.
48. Forsyth WR, Antosiewicz JM, Robertson AD. Empirical relationships between protein structure and carboxyl pKa values in proteins. Proteins 2002;48:388–403.
49. Elcock AH, McCammon JA. Electrostatic contributions to the stability of halophilic proteins. J Mol Biol 1998;280:731–748.
50. Gloss LM, Placek BJ. The effect of salts on the stability of the H2A-H2B histone dimer. Biochemistry 2002;41:14951–14959.